DONNAN POTENTIALS FROM THE A- AND I-BANDS OF GLYCERINATED AND CHEMICALLY SKINNED MUSCLES, RELAXED AND IN RIGOR

E. M. BARTELS AND G. F. ELLIOTT
Biophysics Group, Open University Research Unit, Oxford OX1 5HR, England

ABSTRACT Using a combination of microelectrode measurements and high-power microscopy we have demonstrated that different Donnan potentials can be recorded from the A- and I-bands of glycerinated and chemically skinned muscles in rigor, so that the A-band fixed charge concentration exceeds the I-band fixed charge concentration in the rigor condition. In relaxation the two potentials, and therefore the two charge concentrations, are equal in the two bands. X-ray data are presented for relaxed and rigor rat semitendinosus muscle, chemically skinned, and actin and myosin filament charges are calculated under a variety of conditions. Our conclusions are that (*a*) the fixed (protein) charge is different in the A- and I-bands of striated muscle in the rigor state; (*b*) the fixed charges are equal in the A- and I-bands of relaxed muscle; (*c*) the largest charge change between relaxation and rigor is on the thick filament. This occurs whether or not the myosin heads are cross-linked to the thin filaments. (*d*) Possibly an event on the myosin molecule, the binding of ATP (or certain other ligands) causes a disseminated change that modifies the ion-binding capacity of the myosin rods, or part of them.

INTRODUCTION

The experiments reported in the preceding paper (Naylor et al., 1985) convinced us that different Donnan potentials should arise from the A- and I-bands of glycerinated rabbit psoas muscles in rigor, but that it was impossible to demonstrate these different potentials clearly by "random insertion" microelectrode methods. Here the optical methods used to show these different A- and I-band potentials directly are described, and the observations are extended to glycerinated rabbit muscle in relaxing solution and to glycerinated and chemically skinned rat muscle, both relaxed and in rigor. We wished to investigate possible differences between glycerinated and chemically skinned preparations, and since one of us had experience with rat muscle (Bartels et al., 1979) this was an obvious choice, because it is comparatively easy to dissect small bundles in a relaxing solution without glycerination, a protocol that we found difficult with the classical rabbit psoas muscle.

Here the changes in A- and I-band potentials between relaxed (ATP and EGTA present) and rigor muscles are described. The differences, in a single muscle, between specimens prepared by glycerination and by chemical skinning are also investigated. Preliminary reports of some of these experiments have appeared before (Bartels et al., 1980; Bartels and Elliott, 1980, 1981*a*, *b*, 1982, 1983).

METHODS

Preparations

Chemically Skinned Rat Muscle. Experiments were carried out on the rat semitendinosus muscle. A portion of a fiber bundle, 0.25–0.5 mm in diameter and 10–15 mm in length, was dissected as described for the gracilis muscle by Bartels et al. (1979) in (rat) Ringer's solution, containing (in millimoles per liter): 140 NcCl; 5 KCl; 3.2 $CaCl_2$; 1.1 $MgCl_2$; 4.5 D-glucose; 1.5 phosphate buffer, pH 7. After dissection, the bundle was transferred to relaxing solution, containing (in millimoles per liter): 150 KCl; 5 $MgCl_2$; 5 Na_2ATP (BDH); 4 EGTA; 10 imidazole buffer, pH 7, for 5 min before final transfer to the skinning solution, which was the relaxing solution with the addition of 50 μg saponin ml^{-1}. After 25 min in the skinning solution, the muscle was washed in relaxing solution for 30 min and then transferred to the experimental solution. The fiber bundle was tied into a perspex cell, the sarcomere length was adjusted to the chosen length (using laser diffraction), and the muscle was left to equilibrate for 30 min in the experimental solution before the start of the experiment. The experiments were carried out at a fixed sarcomere length in the range 2.5–3.4 μm, and the sarcomere length was checked at 3–4 points along the length. At longer sarcomere lengths rat muscle does not always show a uniform sarcomere length distribution along the muscle, but in this paper all the results are from preparations with a uniform sarcomere length distribution.

Glycerinated Rat Muscle. Fiber bundles, 1–2 mm in diameter and as long as possible (1–2 cm), were dissected and tied to perspex rods and glycerinated following the procedure for rabbit muscle described by Naylor et al. (1985). Bundles of 2–10 fibers were attached either in a perspex cell or in a petri dish and left to equilibrate in the experimental solution for 30 min before start of the experiment.

Glycerinated Rabbit Muscle. Fiber bundles from the psoas muscle were dissected and glycerinated as described by Naylor et al. (1985) and the experimental procedures were the same as for glycerinated rat muscle.

Experimental Chambers/Cells

A circular perspex chamber was used for all the diffraction experiments and for some of the potential measurements in the chemically skinned rat muscle. The chamber had moveable muscle attachments that made it possible to stretch the specimens when required. The rat specimens were

typically 12 mm long and the chamber had a 9-mm diameter Mylar window in the base, so that diffraction measurements could in principle be made over most of the specimen length. Some of the microelectrode measurements were made in the same chamber, the size was adequate (~26 mm in diameter, 5 mm deep) for an ample volume of bathing solution to be present. As a precaution, if more than two or three microelectrodes were broken in the course of the measurements, the bathing solution was replaced to avoid any possibility of concentration change due to small amounts of 3 M KCl released.

All potential measurements in the glycerinated preparation and in some of the skinned ones were performed in a petri dish. The bottom of the disk was filled to a depth of 2–3 mm with a casting resin (Sylgard-184 [silicone]; Dow Corning Corp., Midland, MI), which when solidified has the consistency of a firm jelly and is biologically inert. A suitable slot (3–4 mm wide, 2 cm long) was cut in this resin, and the single fiber or fiber bundle was stretched between the sides and held by pushing its ends into slots cut in the resin with razor blades.

Solutions

Two series of solutions were used, a rigor series and a relaxing series. The rigor solutions were the same as in Naylor et al. (1985) (see Table I), these are a set of serially diluted ATP-free rigor solutions with decreasing ionic strength. For relaxed muscles the solutions were modified to contain suitable amounts of ATP and also EGTA to chelate calcium ions (Table II). We also made some measurements in solutions of varying pH, keeping the ionic strength constant (Table III). In all our solutions, the concentrations of the free ions were calculated using the Perrin program, see Naylor et al. (1985). The calculated ionic strengths are given in Table I–III.

Microelectrode Measurements

Donnan potentials were measured with the microelectrode techniques described by Naylor et al. (1985). The microelectrodes were filled with 3 M KCl, and the resistance of the microelectrode was monitored at all times using a modification of Naylor's (1978) circuit; readings were discarded if the steady resistance changed by >5% inside the impaled tissue. The microelectrodes resistances were in the range of 14–25 MΩ, which implies that the tip diameters of the electrodes were ~0.1–0.2 μm. Tip potentials were also measured routinely, as described by Naylor et al. (1985), and electrodes with tip potentials >1 mV were discarded. Because we wished to see whether two separate (A- and I-band) potentials could be detected from rat muscles examined by random insertion, some experiments were made by this technique, and the results were displayed as histograms of numbers of readings against observed potentials. Most of our experiments, however, were made under optical observations as described in the next paragraph.

Optical Arrangements

The petri dish or experimental cell with the muscle specimen was placed on the stage of an inverted microscope (model 405; Carl Zeiss, Inc., Thornwood, NY), overall magnification 400 times. A simultaneous combination of phase contrast and polarization contrast was possible with the Zeiss instrument and this was used in all the experiments reported here. Under these conditions of illumination and contrast and with the single fibers, or bundles of a few fibers, there was no difficulty in identifying the A- and I-band regions from the different appearances of the Z-line and H-zone structures at moderate sarcomere lengths.

The method of obtaining contrast proved to be successful with skeletal muscle and the practical resolution was so good that it was possible with confidence to see the position of the microelectrode tip in the A-band or the I-band of slightly stretched muscle fibers (sarcomere length 2.6 μm and above) (Fig. 1), particularly since it was possible to focus up and down to help in locating the tip. At sarcomere lengths ~2.5 μm it was not so easy to locate the tip but it was still just possible. At lower sarcomere lengths it became extremely difficult to see exactly where the tip was placed. Most of our experiments were therefore carried out at sarcomere lengths >2.7 μm, after we had checked that the Donnan potentials were independent of sarcomere length in a particular solution.

The microelectrode was carried on a micromanipulator, which was not mounted on the microscope stage or on the microscope itself, so that the microelectrode could be moved independently of the experimental cell or chamber. The impalement was made using the microscope stage to move the speciment onto the microelectrode, rather than moving the microelectrode into the specimen. The whole apparatus was at ground floor level, and mounted on a massive concrete bench to minimize vibration.

Diffraction Techniques

The methods for x-ray and laser diffraction were as in Naylor et al. (1985). X-ray data for the glycerinated rabbit muscle were taken from their results, but equatorial spacings were measured for the skinned rat muscles. A suitable lid with a second Mylar window was fitted to the specimen cell, which was mounted directly on the x-ray or laser diffraction apparatus as required. When a petri dish was used for microelectrode experiments, sarcomere lengths were determined with a vertically oriented laser beam.

TABLE I
COMPOSITION OF THE RIGOR SOLUTIONS

Rigor solution	KCl	$MGCl_2$	Phosphate buffer, pH 7	Tris-HCl-buffer, pH 6	Ionic strength
	mM	*mM*	*mM*	*mM*	*M*
Standard	100	5	20	—	0.141
2× diluted	50	2.5	10	—	0.072
5× diluted	20	1	4	—	0.030
10× diluted	10	0.1	2	—	0.015
Low pH	50	2.5	—	4	0.074

TABLE II
COMPOSITION OF THE RELAXING SOLUTIONS

Relaxing solution	KCl	$MGCl_2$	Phosphate buffer, pH 7	Na_2ATP (BDH)	EGTA	Ionic strength
	mM	*mM*	*mM*	*mM*	*mM*	*M*
Standard	100	10	20	5	4	0.180
2× diluted	50	5	10	2.5	2	0.180
5× diluted	20	2	4	1	0.8	0.038
10× diluted	10	1	2	0.5	0.4	0.019

TABLE III
COMPOSITION OF THE pH-CHANGE SOLUTIONS AT HIGH AND LOW IONIC STRENGTH

pH solution	KCl	$Mg\ Cl_2$	Citric acid-K_2HPO_4 buffer	Ionic strength
	mM	*mM*		*M*
pH 5.8 low μ	10	0.5	0.8	0.013
pH 4.8 low μ	10	0.5	0.8	0.014
pH 3.95 low μ	10	0.5	0.8	0.014
pH 3.4 low μ	10	0.5	0.8	0.014
pH 5.7 high μ	50	2.5	4	0.066
pH 4.7 high μ	50	2.5	4	0.069
pH 3.7 high μ	50	2.5	4	0.071
pH 3.5 high μ	50	2.5	4	0.073

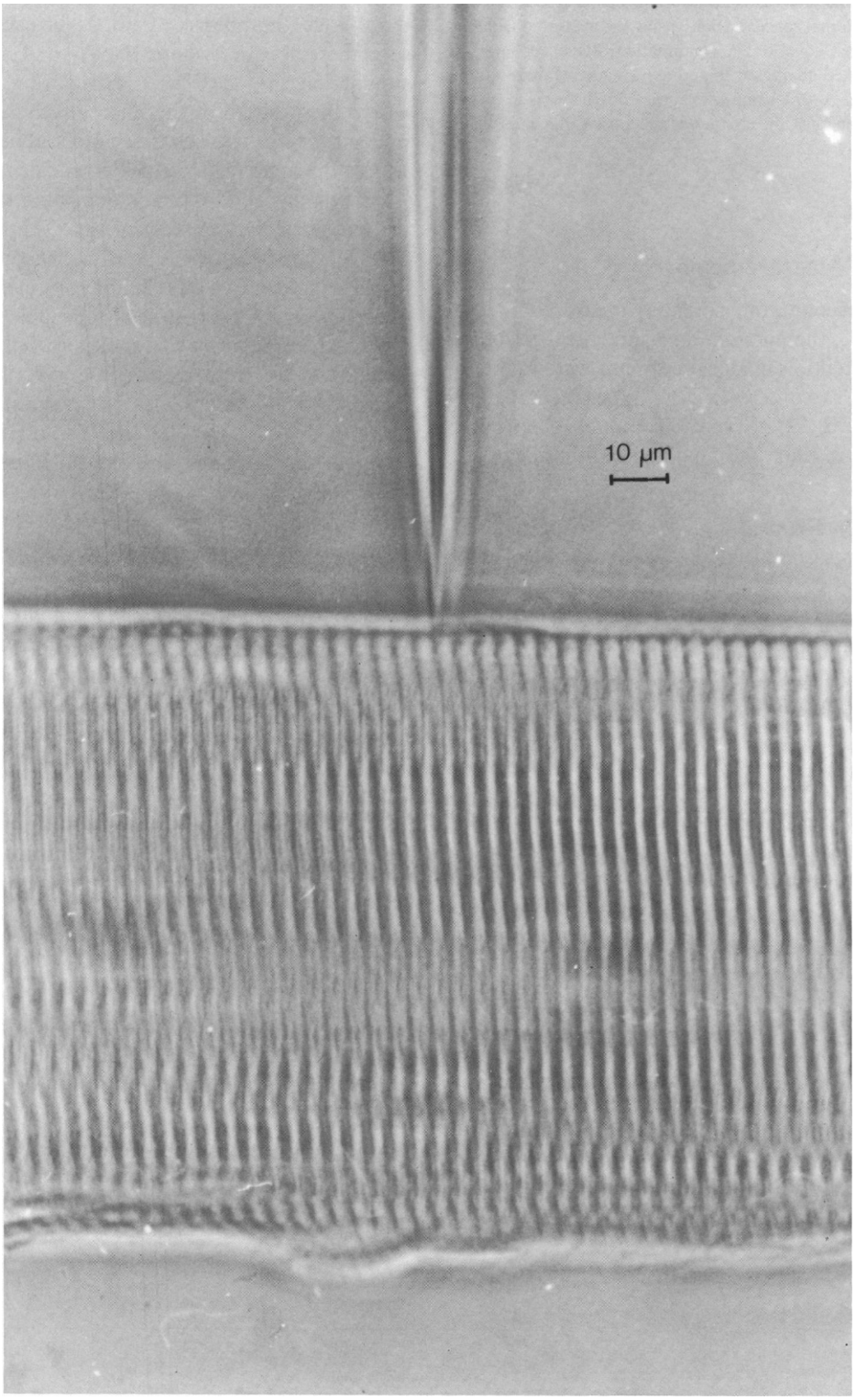

FIGURE 1 Micrograph of bundle of fibers, showing a microelectrode in position in an A-band. The sarcomere length is ~3 μm, the calibration bar is 10 μm.

Theory

The theory was given in Elliott and Bartels (1982), Naylor (1982), and Naylor et al. (1985). The internal concentrations of the free ions were determined from the external concentrations, using the measured Donnan potential and the Nernst equation. A computation of the net internal charge then gave the fixed charge on the protein (filament) matrix, and since the geometry of the A- or I-band was known from the measurements with the diffraction techniques, the charges on the muscle filaments could be determined.

RESULTS

Potential Measurements

In the following account the potential measured in the A-band is called E_A, the potential measured in the I-band is called E_I. The potentials in all experiments were found to be independent of sarcomere length. Experimental data are shown in Fig. 2 for a typical example, chemically skinned rat muscle in rigor and relaxing solutions.

Chemically Skinned Rat Muscle. In random insertion experiments, some of which were made before the set-up was improved with high-power microscopy, two potential peaks were always observed in rigor when 20 readings, taken randomly, were plotted as a histogram. The distribution on the two peaks was dependent on sarcomere length, with fewer readings around the less negative peak at shorter sarcomere lengths and an approximate equal number of readings in each peak at longer sarcomere length (where the A- and the I-band are of similar length), see Fig. 3. Comparing with experiments where the position of the microelectrode is located in the microscope, the less negative potential peak coincides with E_I and the more negative peak coincides with E_A.

In relaxing solutions only one potential peak was found in random insertion experiments. The two potentials E_A and E_I, observed with light-microscope location, were found to be equal in all relaxing solutions. Table IV and V give the data for rat muscle at four ionic strengths, in rigor (IV) and in relaxed (V) conditions. All potential data in the tables are from direct observations under the light microscope. We also made observations in a rigor solution at pH 6 and μ = 0.074 M (see Table III). Data from this solution are included in Table IV and show that in chemically skinned rat muscle, as in glycerinated rabbit muscle, the protein charge concentration in both bands decreases with decreasing pH (above the isoelectric point).

Glycerinated Rat and Rabbit Muscle. There was no significant difference in the potential measure-

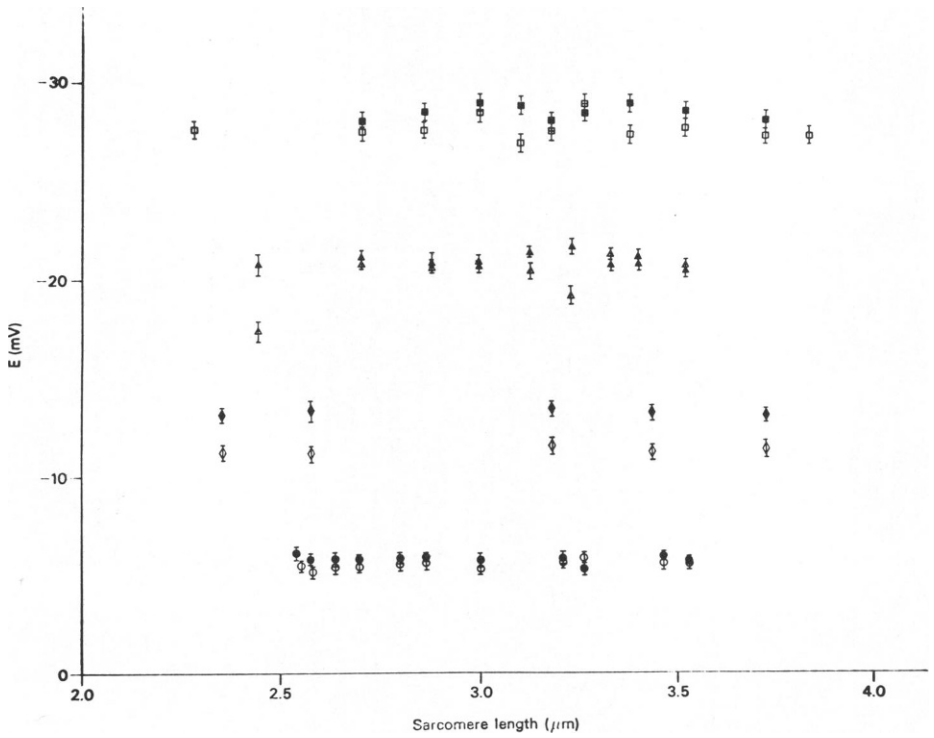

FIGURE 2 Skinned rat muscle, potentials in the various solutions plotted as a function of sarcomere length; standard error shown. Note that in a given solution there is no sarcomere-length variation of potential. These results are from the A-band without Brij treatment and in this band there is no difference between the potentials in relaxation and rigor in these conditions. Solid circles, standard rigor solution; open circles, standard relaxing solution; solid diamonds, 2× diluted rigor solution; open diamonds, 2× diluted relaxing solution; solid triangles, 5× diluted rigor solution; open triangles, 5× diluted relaxing solution; solid squares, 10× diluted rigor solution; open squares, 10× diluted relaxing solution.

ments taken from glycerinated rat fibers and from glycerinated rabbit fibers. E_A and E_I were found to be different and E_A more negative than E_I in all rigor solutions. E_A and E_I were found to be the same in the relaxing solutions. The results are given in Table VI for rat muscle. Notice that in the rigor solution based on 50 mM KCl there was a difference in the values of the potentials between the skinned and the glycerinated muscle. Both the A- and the I-band potentials were significantly more negative in the skinned than in the glycerinated rat preparations. Data for glycerinated rabbit muscle in the relaxing solutions are given in Table VII, and are not very different from the rat data.

In relaxing solution there was a difference between skinned and glycerinated muscle, which was reported in a preliminary communication by Bartels and Elliott (1982). In the glycerinated preparations, E_A decreased from rigor to the relaxed state to a value close to E_I. E_I stayed constant at a given ionic strength. In the skinned muscle E_I increased from rigor to relaxed state to a value close to E_A. E_A stayed approximately constant. We shall return to this point in the Discussion section entitled Rat Muscle—Differences between Skinning and Glycerination.

Naylor et al. (1985) predicted the I-band charge in glycerinated rabbit muscle from experiments on the A-band alone in rigor, varying the ionic strength and the pH. To check these predictions the experiments were repeated measuring the I-band potentials in the solutions used by Naylor et al. (1985). An I-band potential is indeed present (Table VIII) different from the A-band potential in all rigor solutions (compare with Naylor et al., 1985, Tables I and II). The I-band charge decreases with decreasing pH and becomes positive on the acid side of the thin filament isoelectric point.

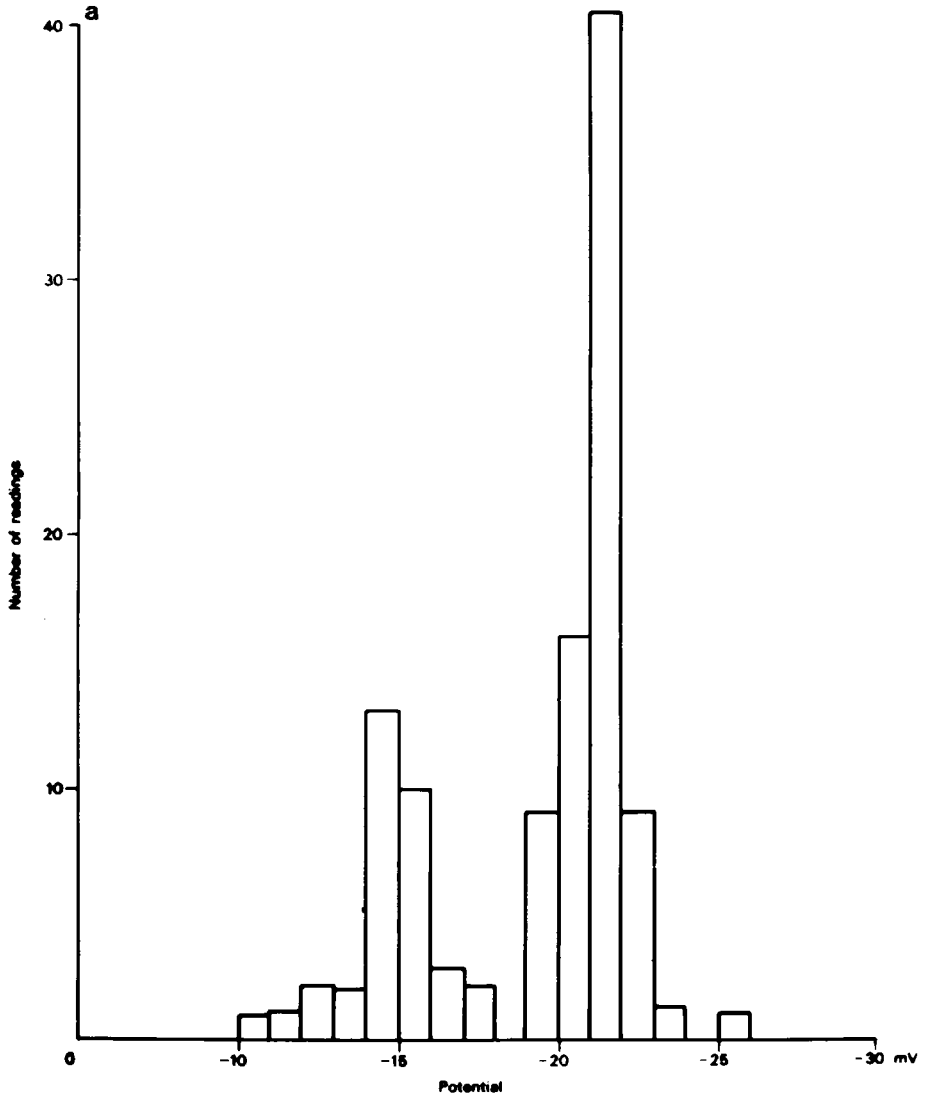

FIGURE 3 Histograms of 20 potentials taken at random (without microscopic observation) in skinned rat muscle in the rigor solution based on 20 mM KCl. Note the different form between long and short sarcomere lengths. (*a*) S = 2.51–2.75 μm; (*b*) S = 3.26–3.50 μm.

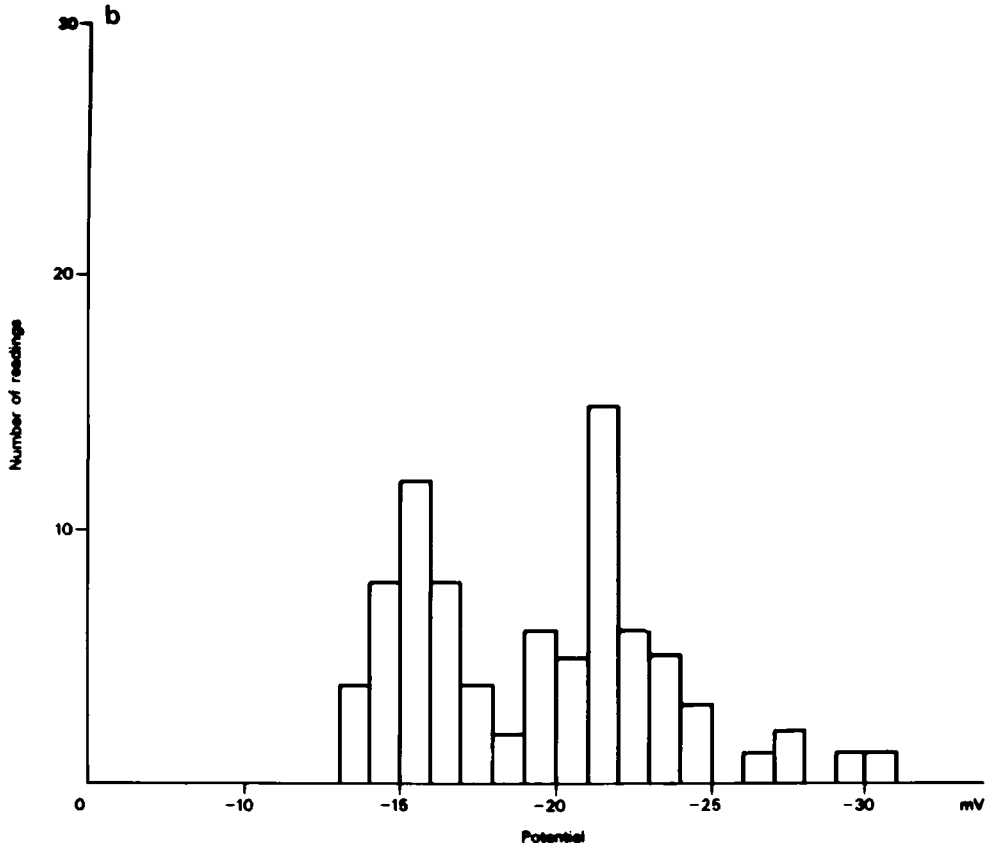

FIGURE 3B

TABLE IV
SUMMARY OF THE RESULTS FROM SKINNED RAT MUSCLE IN RIGOR, INCLUDING ONE SET OF RESULTS AT LOW pH

Solution	E_A	E_I	$[Pr]_A$	$[Pr]_I$	X-ray data	σ_m	σ_a (from x-ray slope)	σ_a (from E_I)	σ_m/σ_a (from x-ray slope)	σ_m/σ_a (from E_I)
	mV	*mV*	*mM*	*mM*		*e/nm*	*e/nm*	*e/nm*		
Standard rigor pH 7 μ = 0.14 M	−5.7 ± 0.6 n = 200	−2.7 ± 0.7 n = 200	−63 ± 7	−30 ± 8	d^* = (50.0 ± 1.0) −(4.4 ± 0.9)S‡ n = 22	51	12	12	4.4	4.2
2× diluted μ = 0.072 M	−11.7 ± 1.0 n = 200	−8.0 ± 0.7 n = 200	−68 ± 6	−46 ± 4	d = (58.1 ± 1.4) −(7.0 ± 1.2)S n=37	47	20	16	2.4	3.0
5× diluted μ = 0.030 M	−19.9 ± 0.9 n = 200	−14.0 ± 0.8 n = 200	−53 ± 3	−35 ± 2	d = (60.3 ± 0.7) −(6.9 ± 1.4)S n=26	43	16	2.7	3.0	
10× diluted μ = 0.015 M	−28.9 ± 1.0 n = 200	−19.6 ± 1.0 n = 200	−44 ± 2	−26 ± 3	d = (59.0 ± 1.2) −(6.2 ± 1.7)S n=15	38	12	11	3.1	3.4
Low pH rigor solution pH 6 μ = 0.074 M	− 8.4 ± 0.5 n = 300	−6.0 ± 0.5 n = 300	−45 ± 3	−32 ± 3	d = (61.1 ± 1.3) −(7.7 ± 2.1)S n=15	32	15	11	2.2	2.8

σ_m and σ_a are the linear charge densities of the thick and thin filaments, respectively. [Pr] is the concentration of protein charge expressed as mM of univalent charge. All potentials and the associated [Pr]s are given as a mean and standard deviation, n is the number of readings. The x-ray data are shown on the least-squares straight line fit to the experimental data, with standard errors calculated in the normal manner. The charge ratio's from the x-ray slope have a precision of about ±50%, the thick filament and thin filament linear charges calculated from the A- and I-band potentials have a precision of about ±20%, and the thin filament linear charge derived from the x-ray slope has much lower precision (see Naylor et al., 1985).

*d is measured in nanometers.

‡S is measured in microns.

X-ray Data

For chemically skinned rat muscle the equatorial (1,0) lattice spacing (d) was determined before the measurement of the potential for 20–25 preparations in each solution. A typical set of data is plotted Fig. 4 for skinned rat muscle in the relaxing solution based on 20 mM KCl.

The spacing shows linear relationships as a function of sarcomere length, decreasing with increasing sarcomere length. For the lowest ionic strength in rigor muscle this is not quite true, however; up to a sarcomere length of 3 μm the regression coefficient for the fitted line fulfills the criteria for a straight line, with d decreasing, but above 3 μm, d stays approximately constant. In this case we have used the equation from the points at or below 3 μm for our present purposes, and we are investigating the phenomenon further. X-ray data for skinned rat muscle, in rigor and relaxed, are given in Tables IV and V.

We are not able to measure stiffness of the fiber in rigor and relaxing solutions because this would have made the apparatus impossibly cumbersome, so as a test for the efficacy of our relaxing solutions we used the relative intensities of the (1,0) and (1,1) equatorial reflections as an index of the state of the muscle (Huxley, 1968; Rome, 1972). Fig. 5 shows the intensity ratio categories (using the scale introduced by Elliott et al., 1963) against sarcomere length for rigor and relaxing solutions. At all ionic strengths the intensity ratio shifts towards the relaxed position of the cross-bridge in the appropriate solution. The value of the lattice spacing, however, did not behave in the same way at all ionic strengths. Comparison of the x-ray data summarized in Table IV and V shows that in the relaxing solution based on 100 mM KCl solution the lattice spacing was generally ~1.5–2.0 nm greater than in the corresponding (rigor) solution, in the solutions based on 50 mM KCl the spacings were about equal, and in the solutions based on 20 and 10 mM KCl the rigor spacing was greater than the relaxed by ~1.0 and 2.0 nm, respectively.

No x-ray data were recorded for glycerinated rat muscles, and the x-ray data for skinned rat muscle in a given solution are used in all calculations where there is no separate set of data. The justification for this is that in our experience, for both rat and rabbit muscles, x-ray equatorial data for skinned and glycerinated preparations are similar in the same solution under all conditions where both sets of data are available.

X-ray data for glycerinated rabbit muscle in rigor are given in Tables I and II of Naylor et al. (1985); for relaxed glycerinated rabbit muscle in our standard relaxing solution we have combined the data of Naylor (1977) and Rome (1972) with the addition of six experimental points taken subsequently. This gives, for the standard relaxing solution based on 100 mM KCl, $d = (56.1 \pm 0.9) - (6.2 \pm 0.7)\ S$ ($n = 74$, units as in Tables IV and V). Notice that the slope of this line is not significantly different from skinned rat muscle in the same solution (Table V) and the difference in the intercepts of the two lines is barely significant.

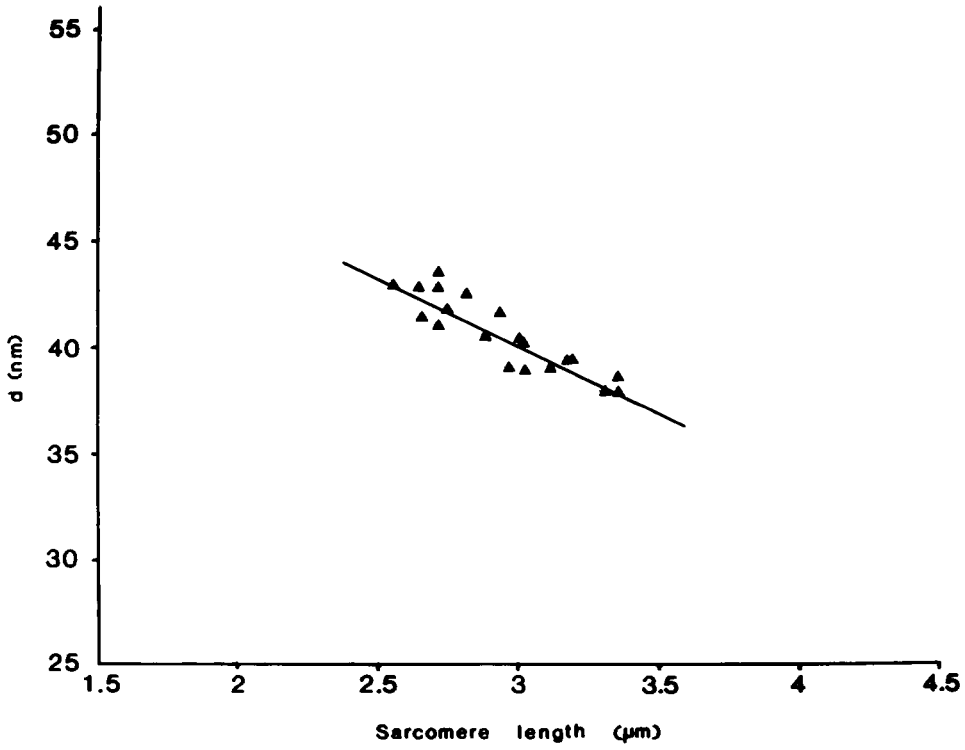

FIGURE 4 A typical set of x-ray data for rat muscle in standard relaxing solution (pH 7, μ = 0.18). The best fit straight line is shown.

TABLE V
SUMMARY OF THE RESULTS FROM SKINNED RAT MUSCLE IN RELAXING SOLUTIONS

Solution	E_A	E_I	$[Pr]_A$ $[Pr]_I$	X-ray data	σ_m	σ_a (from x-ray slope)	σ_a (from E_I)	σ_m/σ_a (from x-ray slope)	σ_m/σ_a (from E_I)
	mV	*mV*	*mM*		*e/nm*	*e/nm*	*e/nm*		
Standard relaxing				d^* = (59.1 ± 0.9)					
pH 7	−5.0 ± 0.8	−5.0 ± 0.8		−(6.4 ± 1.4)S‡	(59)	(20)	(30)	3.0	2.0
μ = 0.18M	n = 200	n = 200	−70 ± 11	n = 22					
2× diluted	−9.2 ± 0.9	−9.1 ± 1.0		d = (53.0 ± 1.0)					
μ = 0.086M	n = 200	n = 200	−65 ± 7	= −5.5 ± 1.3)S	(47)	(15)	(24)	3.2	2.0
				n = 19					
5× diluted	−19.5 ± 1.0	−19.6 ± 1.0		d = (59.9 ± 0.9)					
μ = 0.038M	n = 200	n = 200	−62 ± 4	−(7.4 ± 1.6)S	(44)	(19)	(22)	2.3	2.0
				n = 22					
10× diluted	−27.4 ± 1.0	−27.3 ± 0.9		d = (58.2 ± 1.1)					
μ = 0.019M	n = 200	n = 200	−49 ± 3	−(6.4 ± 1.4)S	(39)	(14)	(20)	2.9	2.0
				n = 24					

The charge values from the A- and I-band potentials are given in parentheses because it seems likely that these include SR values as well as filament effects (see text). Other details as Table IV.
*d is measured in nanometers.
‡S is measured in microns.

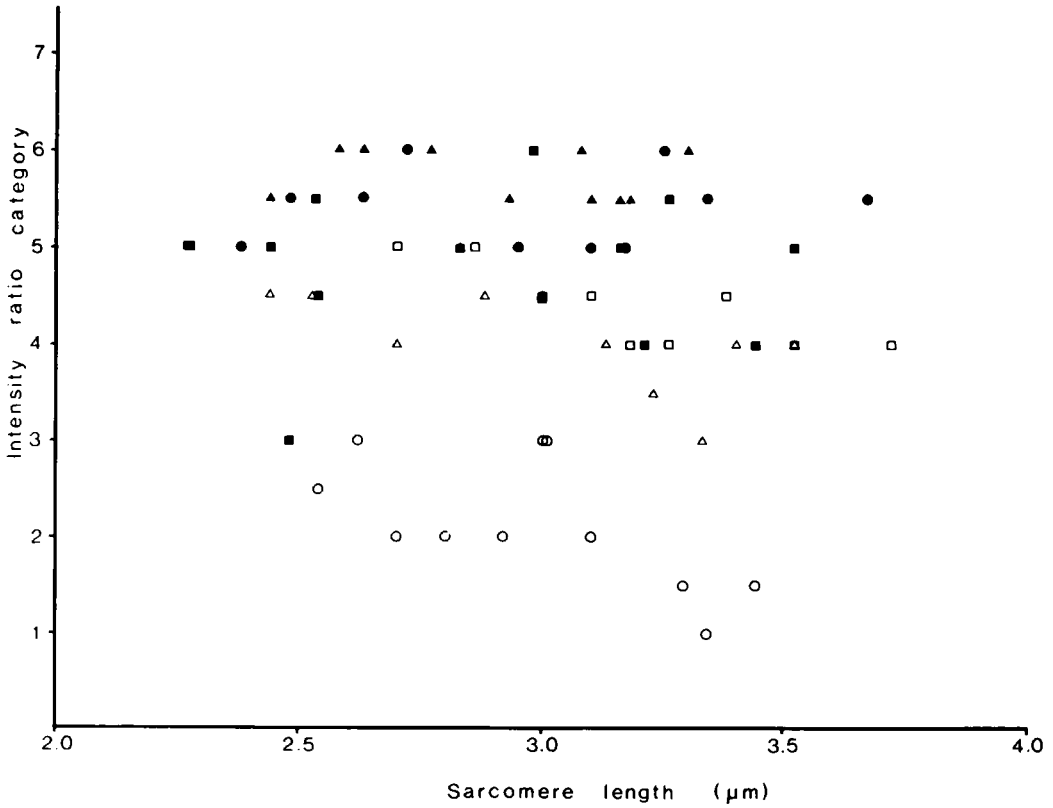

FIGURE 5 The relative intensities of the (1,0) and (1,1) equatorial reflections in relaxation and rigor as a function of sarcomere length. The qualitative scale used is taken from Elliott et al. (1963), and uses the following categories: (*a*) 1,0 seen clearly, no sign of 1,1; (*b*) 1,0 seen clearly, traces of 1,1; (*c*) 1,0 > 1,1, both seen clearly; (*d*) 1.0 ≃ 1.1, both seen clearly; (*e*) 1.0 < 1.1, both seen clearly; (*f*) traces of 1.0, 1.1 seen clearly; (*g*) no sign of 1.0, 1.1 seen clearly. Other symbols as in Fig. 2, open symbols are in relaxed muscle, solid symbols in rigor, circles are standard solutions, triangles 5× diluted, and squares 10× diluted. Notice that the intensity ratio shows appropriate changes between the rigor and relaxing solutions, at all dilutions and at all sarcomere length.

TABLE VI
POTENTIALS AND CHARGE VALUES FROM GLYCERINATED RAT MUSCLE

Solution		E_A	E_I	$[Pr]_A$		$[Pr]_I$
		mV	*mV*	*mM*		*mM*
Standard	rigor	−5.3 ± 0.5	−2.7 ± 0.6	−59 ± 5		
	relaxing	−2.5 ± 0.5	−2.6 ± 0.6			
					−36 ± 7	−30 ± 6
2× diluted	rigor	−8.6 ± 0.7	−5.2 ± 0.7	−49 ± 4		
	relaxing	−5.2 ± 0.6	−5.2 ± 0.7			
					−37 ± 3	−29 ± 4
5× diluted	rigor	−20.4 ± 0.9	−13.0 ± 0.9	−54 ± 3		
	relaxing	−12.9 ± 1.0	−12.9 ± 1.0			
					−39 ± 3	−32 ± 2
10× diluted	rigor	−27.1 ± 1.0	−20.1 ± 1.0	−40 ± 2		
	relaxing	−20.1 ± 1.0	−19.9 ± 1.0			
					−32 ± 2	−27 ± 2

Standard deviations shown. [Pr] defined as in Table IV.

Calculations of Filament Charge

The protein charge concentration [Pr] was calculated in each case (Elliott and Bartels, 1982) and the results are given in Table IV–VIII.[1] The net charge per nanometer of filament was calculated using the diffraction data to determine the relevant volumes, these charges are also given in Tables IV, V, VII, and VIII. The thin filament charge is seen to be essentially constant over the range of ionic strengths, the thick filament charge increases with ionic strength.

DISCUSSION

Relaxation and Rigor — Thick Filament Charges

In relaxed muscle, an excess of Mg-ATP is present in solution and pCa is held >7 by a chelating agent. The myosin heads are free to move, and are in thermal motion about their equilibrium positions (Poulsen and Lowy, 1983). In rigor muscle there is no free ATP, and the myosin heads are very probably bound to the actin filaments in the overlap zone; the x-ray evidence for this statement is well reviewed in Hanson (1968). It has often been suggested (e.g., Reedy et al., 1965; Hanson, 1968) that the rigor conformation represents a frozen state of the myosin heads in one phase of the contractile cycle. Although Huxley (1973) pointed out that the x-ray pattern of contracting muscle does not resemble that of rigor muscle to any large extent, it is likely that rigor muscle is related to contracting muscle, so that information about muscle in rigor may be relevant to the contraction mechanism.

The first measurements of Donnan potentials in relaxed (glycerinated rabbit psoas) muscle were made by Pemrick and Edwards (1974). In this pioneering study they reported a sarcomere-length effect in relaxation though not in rigor (their Figs. 2 and 3); this sarcomere-length effect is not seen in the present measurements. However, their experimental data are not convincing on this point, because the values of potential that they report do not accord with our own, theirs being considerably more negative both in relaxation and in rigor in the same muscle in similar solutions at similar ionic strengths. Possibly they may have been affected by the microelectrode artefact, which was described in Naylor et al. (1985). Note that the tip size of their microelectrodes (~1 μm) was 5–10 times greater than those used here (Naylor et al., 1985) and it is therefore possible that their electrodes averaged the potentials differently from those used here. Our experience is that there is no sarcomere length effect on the A-band or I-band potentials, either in relaxation or in rigor (i.e., Fig. 2). This statement includes observations made in solutions identical with those used by Pemrick and Edwards (1974).

The explanation for the lack of sarcomere-length effect given by Elliott et al. (1978) and see also the preceding paper, Naylor et al. (1985), is that the volume of the A-band phase increase as extra charge is brought into the A-band by the thin actin-containing filaments, and that this volume change compensates for the extra charge, so that the average charge concentration in the A-band, which will determine the observed potential, stays constant. This explanation is very similar to that given by

[1]Here also it is convenient to express protein charges in millimoles per liter prime (mM′) of univalent charge, see Naylor et al. (1985).

TABLE VII
SUMMARY OF RESULTS FROM GLYCERINATED RABBIT MUSCLE IN RELAXING SOLUTIONS

Solution	E_A	E_I	$[Pr]_A$ $[Pr]_I$	X-ray data	σ_m	σ_a (from x-ray slope)	σ_a (from E_I)	σ_m/σ_a (from x-ray slope)	σ_m/σ_a (from E_I)
	mV	*mV*	*mM*		*e/nm*	*e/nm*	*e/nm*		
Standard relaxing pH 7 μ = 0.18M	−2.3 ± 0.6 n = 400	−2.2 ± 0.7 n = 400	−31 ± 9	d^* = (56.1 ± 0.9) −(6.2 ± 0.7)S‡ n = 74	23	8	12	2.8	2.0
2× diluted μ = 0.086M	−6.0 ± 1.0 n = 400	−5.7 ± 1.0 n = 400	−42 ± 7	d = (53.0 ± 1.0) = −(5.5 ± 1.3)S n = 19	30	9	15	3.2	2.0
5× diluted μ = 0.038M	−14.8 ± 1.1 n = 400	−14.8 ± 1.1 n = 400	−45 ± 4	d = (59.9 ± 6.9) −(7.4 ± 1.6)S n = 22	32	14	16	2.3	2.0
10× diluted μ = 0.019M	−19.8 ± 1.1 n = 400	−19.5 ± 1.0 n = 400	−32 ± 2	d = (58.2 ± 1.1) −(6.4 ± 1.4)S n = 24	26	9	13	2.9	2.0

Other details as in Table IV.
*d is measured in nanometers.
‡S is measured in microns.

Elliott (1973) to explain the roughly linear behavior of the (1,0) x-ray spacing with muscle length in glycerinated and skinned muscles. The explanation implies that the microelectrode responds to the average ionic concentration (or potential, see Elliott and Bartels, 1982) within the whole A-band, and does not respond to the local concentrations in the H-zone or overlap regions where the tip finds itself. This suggests that the microelectrode tip, although only 0.1–0.2 μm in diameter, nevertheless has a response field that is probably a single order of magnitude larger than this. Certainly, as was pointed out in the previous paper, it has not been possible to detect separate potential regions in the H-zone and overlap regions, see also Fig. 2.

Aldoroty et al. (1985) in their investigation of crayfish muscle fibers, where the A-band is three times longer than rat or rabbit muscle, have observed a small sarcomere-length effect on the A-band potential. In this muscle there are six thin actin-containing filaments for every thick myosin-containing filament, so the charge brought into the A-band as the overlap increases is considerably larger than in rat and rabbit muscle where there are only two thin filaments per thick filament. Possibly in these circumstances the volume change in the A-band is unable to compensate for the extra charge, so that the charge concentration, and thus the A-band potential, does increase with sarcomere length decrease.

The major observation of this paper is that for both rat and rabbit muscle it is possible to record Donnan potentials

TABLE VIII
I-BAND POTENTIALS AND CHARGES FOR GLYCERINATED RABBIT MUSCLE IN RIGOR SOLUTIONS

Solution	E_I	[Pr] (mM) σ_a (e/nm)	Solution	E_I	[Pr] (mM) σ_a (e/nm)	Solution	E_I	[Pr] (mM) σ_a (e/nm)
	mV			*mV*			*mV*	
Rigor series		−29 ± 5	pH series, low μ		−6.3 ± 1	pH series, high μ		−25 ± 3
pH 7.0	−2.6 ± 0.5	13	pH 5.8	−5.8 ± 0.5	2	pH 5.7	−4.6 ± 0.6	9
μ = 0.14 M	n = 400		μ = 0.013 M	n = 80		μ = 0.066 M	n = 80	
pH 7.0	−5.4 ± 1.0	−31 ± 6	pH 4.8	−4.7 ± 0.6	−4.6 ± 1	pH 4.7	4.6 ± 0.6	26 ± 4
μ = 0.072	n = 400	13	μ = 0.014 M	n = 80	1	μ = 0.069 M	n = 80	11
								net positive charge
pH 7.0	−14.5 ± 1.1	−36 ± 3	pH 3.95	6.9 ± 0.6	9 ± 1	pH 3.7	6.8 ± 0.5	42 ± 4
μ = 0.030	n = 400	13	μ = 0.014 M	n = 90	2	μ = 0.071 M	n = 80	19
					net positive charge			net positive charge
pH 7.0	−18.8 ± 1.5	−25 ± 2	pH 3.4	15.1 ± 0.7	27 ± 3	pH 3.5	10.1 ± 0.6	73 ± 6
μ = 0.015	n = 400	9	μ = 0.014 M	n = 80	7	μ = 0.073 M	n = 80	21
					net positive charge			net positive charge

Values are measured for comparison with derived values in Naylor et al., 1985. Other details as in Table IV.

TABLE IX

A- AND I-BAND POTENTIALS, IN STANDARD RIGOR AND RELAXING SOLUTIONS, FROM CHEMICALLY SKINNED RAT MUSCLES TREATED WITH 500 μg ml^{-1} BRIJ 58 SOLUTION IN THE SKINNING SOLUTION FOR 35 min TO INACTIVATE SR

	E_A	E_I
Standard rigor solution	-5.4 ± 0.7 ($n = 120$)	-2.4 ± 0.6 ($n = 120$)
Standard relaxng solution	-2.5 ± 0.7 ($n = 80$)	-2.4 ± 0.6 ($n = 80$)

The A- and I-band potentials, under these conditions, conform to the pattern seen in glycerinated rat muscle (Table VI) rather than in chemically shinned rat muscle without Brij treatment (Tables IV and V). Standard deviations are shown. n is the number of readings.

from the A- and I-bands separately and directly. In rigor the A-band potential, E_A, is significantly more negative than the I-band potential, E_I. In relaxation the two potentials are equal within the experimental error and their value is close to E_I measured in rigor. (The last part of the second statement does not apply to chemically skinned rat muscle in relaxing solution; we will comment in the next section on the difference between the results for skinned and glycerinated muscle in relaxing solutions.) This clear observation of an A-band potential, which is more negative in rigor than in relaxation, means that the lattice electric charge in the A-band is significantly higher in rigor than in relaxation (after making proper allowance for any observed volume changes).

How much higher is the A-band protein charge in rigor? This depends on the solutions that are compared. Taking the rigor and relaxing solutions, both based on 100 mM KCl, the values are 53 mM in rigor and 33 mM in relaxation, an increase of ~60% in rigor. However, the relaxing solution has a greater ionic strength than the rigor solution (Tables IV and V) because of the added ions. In Fig. 6 the A- and I-band protein charges for rabbit muscle are plotted as a function of ionic strength. At a constant ionic strength of 0.14 M appropriate for mammalian muscle, the A-band charge is 53 mM in rigor and 38 mM in relaxing solution, an increase of ~40% in rigor. Whichever of these increases may be appropriate in the physiological case, the increase is too large to be explained by the binding of two ligands (ATP, for example) to the myosin molecule. Taking the lower of the two figures, if the net myosin charge in relaxation is ~80–90 electrons (e)/molecule (Milhayi, 1950, Jennison et al., 1981, and Karn et al., 1983, all give values close to this range), then the extra charge in rigor is 32–36 e, too large for two ATP molecules (~6–8 e). In addition, in relaxed muscle these ligands are supposed to be bound, and to be released when

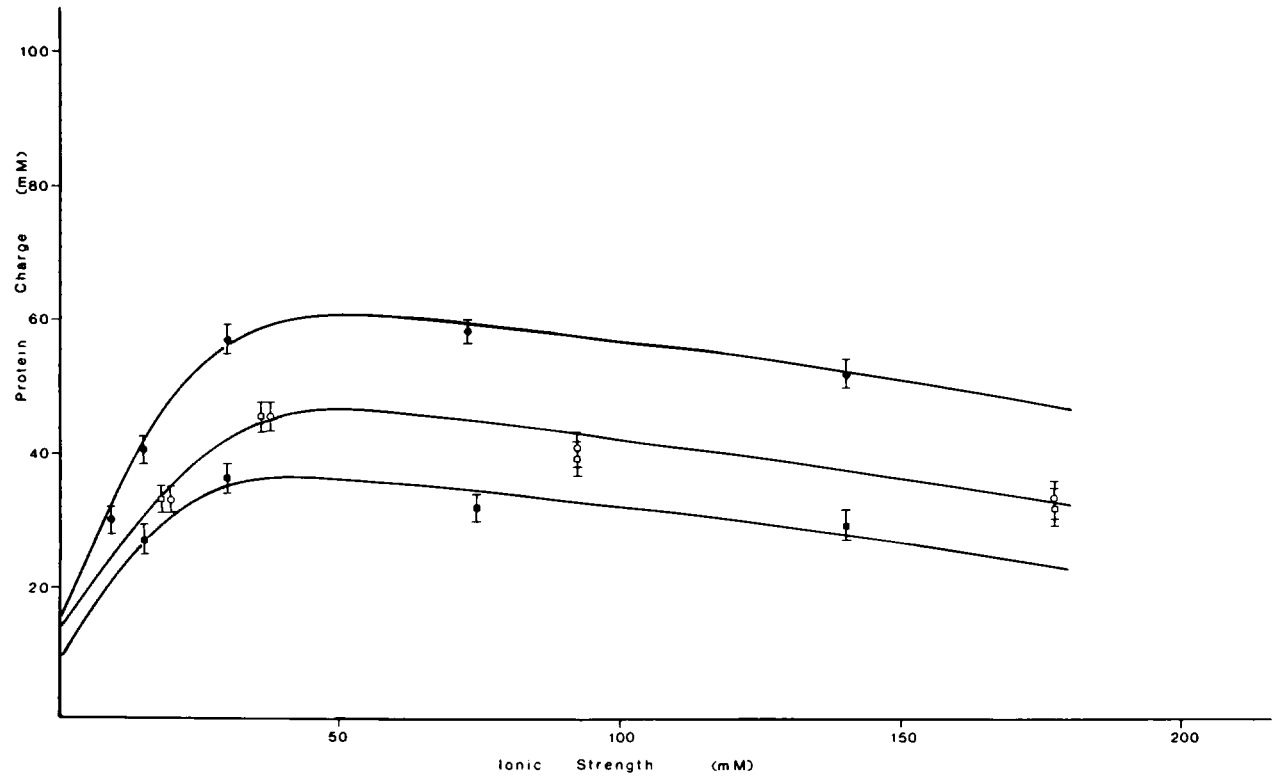

FIGURE 6 The protein charge in glycerinated rabbit psoas muscle, relaxed and in rigor, as a function of ionic strength. Standard deviations shown, number of readings $n = 400$ for each point. Solid circles, A-band, rigor; open circles, A-band relaxed; solid squares, I-band, rigor; open squares, I-band relaxed.

the muscle goes into the contraction cycle and presumably into rigor also, an effect that would be in the reverse direction to our observation. The implication is that the charge effect must be amplified in some way, and we shall return to this point in the section entitled Charge Amplification.

There is a further implication of our results and those of Naylor et al. (1985). Since the extra charge in rigor is not a function of sarcomere length, and thus not a function of filament overlap, the effect cannot depend primarily on actin-myosin cross-linking unless a very few cross-links are sufficient for total charging. It seems then that in rigor there may be two quite separate effects, the myosin-containing filaments charge up throughout the A-band, and they cross-link to the actin filaments in the overlap region. These effects both depend on the absence of free ATP, but the charging effect may occur independently of cross-linking.

Scordilis et al. (1975) used the fluorescent dye CC-6 to serve as an indicator of the potential measured in glycerol-extracted muscle with microelectrodes, and showed that the fluorescence decreased by ~30% on the addition of ATP. They did not then localize this effect, but Scordilis, S. P. (unpublished results), using synthetic thick and thin filaments showed that the effect was primarily due to the myosin-containing filaments. This work correlates closely with the present observations.

Rat Muscle — Differences between Skinning and Glycerination

In chemically skinned rat muscle, different behavior to glycerinated rat muscle was observed. For both preparations in rigor, E_A is significantly greater than E_I and in relaxation the two potentials are equal within experimental error. Except in the solution based on 50 mM KCl (see the section entitled Potential Measurements in Results) the rigor results from the two preparations are not significantly different, but in the glycerinated preparations, E_A decreases in relaxation to E_I (rigor), whereas in the skinned preparations, E_I increases in relaxation to E_A (rigor), see Tables IV–VI. We found this difference puzzling, and it seemed that it could be explained most simply by another structure, in parallel with the whole sarcomere, which charged up (negatively) as the myosin-containing filaments discharged, and vice versa. Since this structure would appear to be effective in skinned preparations but not in glycerinated ones, an obvious candidate is the sarcoplasmic reticulum (SR), because the main difference between the two preparations could be the lack of an effective SR in the glycerinated case. It is therefore suggested that the different behavior of the two preparations might be caused by charging the longitudinal elements of the SR in relaxation, probably by phosphate compounds absorbed to the outer surface. This hypothesis was tested (Bartels and Elliott, 1982) by treating skinned fibers with a 500 μg/ml Brij 58 solution for 35 min to inactivate the SR (Orentlicher et al., 1974). As predicted, these muscles then gave similar results to glycerinated muscle (Table IX). Potential measurements are difficult in the Brij-treated muscles because the electrode tip tends to block, possibly with pieces of SR.

The hypothesis may be made quantitative by considering the fixed charge concentrations in the two bands. In the solutions based on 100 mM KCl, for glycerinated relaxed both are -36 ± 8 mM, and for skinned relaxed both are -70 ± 11 mM, so the SR contribution, according to our hypothesis, is about -34 mM. The total surface area per unit volume of the S has been estimated (for frog muscle) to be ~2.0 μm^{-1} of fiber (Mobley and Eisenberg, 1975). Combining these figures gives a charge change of ~ 10 e nm^{-2} of SR membrane. This figure seems plausible, but suggests that the hypothetical charging is not simply the binding of ATP at the ATPase sites. This would require about three ATP molecules per square nanometer, while the x-ray studies of Worthington and Liu (1973) show that ATPase particles in SR membranes are ~7 nm apart. It is therefore necessary to invoke some as yet unspecified effect of the Ca-ATP membrane pump, and of the ions that have been pumped into the SR. A very similar behavior to that in the chemically skinned rat muscles has also been observed in mechanically skinned barnacle muscles (Bartels and Elliott, 1981*b*). These barnacle muscles also have a well-developed SR system (Selveston, 1967) and the same considerations probably apply as in rat muscles. Aldoroty and April (1984) have also observed effects that they ascribe to membrane charging. Although the hypothesis has been developed by considering the SR, it remains formally possible that another parallel system might be involved. The cytoskeleton is an obvious alternative candidate.

Thin Filament Charge, the Effects of ATP, Ionic Strength, and pH

The thin filament charge measured in the I-band changes between the ATP-free rigor solution and the ATP-containing relaxing solution. From Fig. 5, at $\mu = 0.14$ M, the change is from about -28 mM (rigor) to about -38 mM (relaxing). This corresponds to an increase of (negative) charge of ~5 e/actin monomer in the thin filament, and might be the binding of two phosphate ions per monomer (in a recent preliminary communications, El-Salch and Johnson [1982] have suggested that actin can bind up to nine phosphate ions noncovalently). The thin filament charge also changes with ionic strength (Fig. 5) and with pH (Tables IV and VIII).

The thin filament charges measured in the I-band can be compared with those predicted from the A-band charge using the method of Naylor et al. (1985). The values in Table VIII, for both ionic strength and pH variation, may be compared with those in Tables I and II of Naylor et al.

(1985). There is reasonable agreement in the ionic strength series, and in the low μ pH series at all pHs except pH 3.5, if it is assumed that because of the uncertainty in Naylor et al.'s method of prediction a factor of two difference between the two figures is acceptable. In the pH series at high μ the agreement is not within this criterion, and the predicted charge is much smaller than that measured in the I-band. This might imply that in such rigor solutions negative ions are lost from the actin-containing filaments when they cross-link to the myosin heads (or alternatively that more positive ions bind). Alternatively, and more likely, the disagreement may indicate that the Naylor et al.'s method is not a good one where the gradient term in the x-ray data is <3.0 (in the units defined by the equation) because the uncertainty in the spacing difference between $S = 2.2$ μm and $S = 3.8$ μm is then too great. In relaxing solutions the thin filament charge in glycerinated rabbit muscle predicted from the A-band spacing variation is in reasonable agreement with that directly measured from the I-band potential (Table VII). This is also true of the results from skinned rat muscle in rigor (Table IV). In both these cases the gradient terms are >3.0. It is concluded that in skinned and glycerinated preparations the gradient of the d vs. S relationship of the x-ray data can be used to indicate the relative charges on the thick and thin filaments, as suggested by Elliott (1973) and Naylor et al. (1985), except when the gradient term is <3.0 in the units defined by the equation.

Charge Amplification

The charge amplification effect, which appears as a firm conclusion from these experiments (see the Relaxation and Rigor — Thick Filament Charges section above) leads immediately to a question, exactly where in the thick filament does this amplification occur? It seems very probable that it must involve the myosin molecules themselves, since these are the major constituent of thick filaments, and since the work of Scordilis, S. P. (unpublished results) also suggests this. We are currently seeking to confirm this with experiments on threads made from purified myosin molecules (Cooke et al., 1984; Bartels et al., 1985). On the assumption that it is so, where in the myosin molecule, or the assembly of myosin molecules, does the charge amplification reside?

At the present time any answer to this question must of necessity be hypothetical. There are, however, a number of clues. The amino acid sequence data of McLachlan and Karn (1982) and Karn et al. (1983) leads to a net charge of 2 e^+ on the heavy chain of each myosin head, if the 21 histidine residues are not ionized. On the rod portion of the molecule the net charge is 94 e, if the 34 histidine residues are not ionized; thus the net molecular charge (excluding the light chains) is 90 e (two heads and one rod). Notice that the major part of the molecular charge is one the rod, the heavy chains of the myosin heads are comparatively neutral at physiological pH. Lowey et al. (1969) observed by chromotographic elution that the head was less negatively charged than the rest of the myosin molecule.

It is possible that the extra charge in rigor appears on the head alone, and that the head charge increases from 2 e^+ to 16 e to accommodate an extra 18 e per head (see the Relaxation and Rigor — Thick Filament Charges section above). This seems a very large increase to be accommodated in a comparatively small globular protein, and no obvious physical model comes to mind. As has already been explained this could not be just the effect of binding one ligand molecule (ATP or ADP) per head.

A second possibility is that the head charge stays the same or nearly the same, and the extra charge is distributed uniformly along the rod. McLachlan and Karn (1982) have shown that in a myosin rod there are 38 repeat sequences of 28 amino acids, showing a similar and pronounced charge pattern in each sequence. The charged state, which has been observed, would on this basis be about one extra electronic charge for each of these 38 sequences. As a third possibility, the change might be confined to the S_2 region of the myosin molecule, the first 12 of these sequences. In this case the extra charge per sequence would be ~3 e, which looks interestingly as though it might be one phosphate ion (though the numerology should not be taken too seriously, for the whole rod only one in three sites might be occupied, each with a phosphate ion).

The latter two models have a common mechanism, the binding of ATP to myosin (which is the major effect in relaxation) causes the release of ions from the myosin rod or at least from part of it. How could this occur? For a possible mechanism, attention may be drawn to the views of Saroff (e.g., Loeb and Saroff, 1964) who considers that ion binding to proteins takes place by hydrogen bonds onto networks of charged side chains clustered along the polypeptide chain (Fig. 7). In myosin such clusters, which have been called "Saroff sites," may be set up between the myosin molecules in the filament (Elliott, 1980) or possibly, in view of the sequence data of McLachlan and Karn (1982), between the two polypeptide chains in one myosin molecule. In either case, mechanical stress transmitted along the shafts of the molecules, or between the two chains in a single molecule, might make small alterations in the structure of the intermolecular, or interchain Saroff sites. Saroff (1973) discussed "linked sites," which give rise to cooperativity in ion binding; we have observed (Elliott, 1980; Bridgman, T. D., E. M. Bartels, and G. F. Elliott, manuscript in preparation) that the ion-binding effects in muscle A-bands do appear to be cooperative.

Extended salt-bridge networks have been demonstrated in crystallographic studies by Bloomer et al. (1978) between the subunits of tobacco mosaic virus (TMV) coat protein, and by Adams et al. (1973) in lactate dehydrogenase. In the latter study the networks were specifically identified as anion binding sites. Perutz (1978) gives other

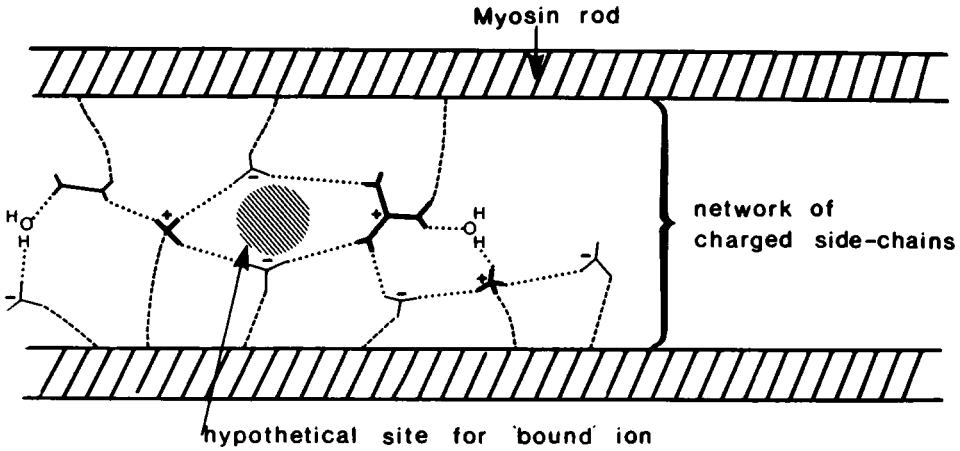

FIGURE 7 A hypothetical Saroff site, a network of charges side chains between two myosin rods (or possibly between two myosin polypeptide chains in a single myosin rod). The binding of some ion to such a site would affect the local charge balance, and this might cause a disseminated mechanical strain in the rod or rods, which might affect the binding properties of a similar neighboring binding site, possibly cooperatively. Notice that the vertical scale between the rods has been much exaggerated to show the network. In all probability the site is much more compact than it appears in this diagrammatic representation.

examples of extended salt-bridge interactions, and draws attention to their probable involvement in the allosteric interactions of hemoglobin. In a recent review of methods of reconstructing myosin filaments from solution, Koretz (1982) stresses the importance of pH and precise ionic conditions, which will control the molecular charge, and probably the ion-binding capacity, of the filaments formed.

It would not be appropriate to go further into these matters in this paper, so we will merely suggest the tentative model shown in Fig. 7. The interactions of myosin with ATP/ADP, by transmitting stress along the rod, controls the ion-binding characteristics of the rods, or of part of them. To explain the present results the binding of ATP would cause the low-charge state, its release would cause the high-charge state. Preliminary experiments have shown (Bartels and Elliott, 1983) that PP_i also gives the low-charge state, while ADP and AMP-PNP give the high-charge one.

This mode of action would fit easily into models of muscle contraction of the type envisioned by Harrington et al. (1979) though it would also fit easily into models of the swelling type (Elliott et al., 1970, see also the discussion after the paper of Elliott et al., 1978). Current work on myosin threads (Cooke et al., 1984; Bartels et al., 1985) is aimed at clarifying the details of the mode of action.

CONCLUSIONS

(*a*) The fixed protein charge is different in the A- and the I-bands of striated muscle in the rigor state. (*b*) The fixed charges are equal in the A- and I-bands of relaxed muscle. (*c*) The largest charge change between relaxation and rigor is on the thick filaments, and occurs whether or not the myosin heads are cross-linked to the thin filaments. (*d*) Possibly an event at one position on the myosin molecule, the binding of ATP (or certain other ligands) causes a disseminated change that modifies the ion-binding capacity of the myosin rods or parts of the them.

APPENDIX

Discussion of Postulated Diffusion Potentials in the Presence of ATP

It has recently been suggested that there is a substantial contribution from diffusion potentials, particularly in the presence of ATP, which affect the measured Donnan potential (Godt and Baumgarten, 1984). We have commented already on these experiments (Elliott et al., 1984) but would like to give a quantitative calculation here.

The concentration of myosin heads in a typical A-band is ~0.4 mM and at the height of activation each head hydrolyzes ~35 ATP molecules/s. Therefore in a contracting muscle A-band the turnover of ATP and its product is ~14 mM/s. It is more difficult to know what is the ATP turnover in a relaxed muscle, but it is probably a factor of 10 or 100 times smaller. De Simone (1977) used the Nernst-Planck diffusion equation to calculate the deviations from equilibrium (Donnan) potentials. The deviation potential was governed by a dimensionless coefficient, μ, which he defined in his Eq. 21.

$$\mu = \frac{J_r}{Kc}\left(\frac{1}{D_2} - \frac{1}{D_1}\right).$$

Here J_r is the flux of reactants, K is the Debye-Hückel constant, c is the reservoir ion concentration, and D_1 and D_2 are the diffusion coefficients of the reactant and product.

This equation can be applied to the diffusion of ATP and its products in the muscle case. If cylindrical geometry and radial flow are assumed the flux of the reactants in contracting muscle is $14 \times r/2$ mM·s^{-1} per unit area, where r is the cylinder radius. (For spherical geometry the factor is $r/3$, the difference is trivial.) The diffusion coefficients for ions in muscle were measured by Kushmerick and Podolsky (1969) who gave ~0.2×10^{-5} cm^2 s^{-1} for ATP and ~0.4 in the same units for SO_4 (this is probably similar to PO_4, which they did not measure). In our experiments the reservoir ionic strength is 180 mM in standard relaxing solution, and the Debye-Hückel constant at this ionic strength is of the order 10^7 cm^{-1}.

De Simone's coefficient in these circumstances is $\mu \sim (14/10^7 \times 180) \times 10^5 \times (2.5 - 5) \times (r/2)$ (working in centimeters, seconds, and

millimoles) $\sim -1 \times 10^3 r$. If r is taken as the myofibrillar radius ($\sim 10^{-4}$ cm), this coefficient is of order 10^{-7}, if as the fiber radius ($\sim 10^{-2}$ cm), the coefficient is of order 10^{-5}. In either event De Simone's analysis shows that the deviations from the equilibrium potential are negligible for contracting muscle, and thus even more so for resting muscle.

We have already demonstrated (Elliott and Bartels, 1982, and in the previous paper, Naylor et al., 1985) that the KCl diffusion potentials are within the experimental error the same inside and outside the muscle lattice, and therefore cancel out in the Donnan potential measurement. It can be concluded that diffusion potentials, either passive diffusion potentials from KCl or active diffusion potentials from metabolically used ATP, are negligible in the experimental measurements of Donnan potential described in this paper.

We are grateful to Professor B. M. Millman, Ms. Katy Jennison, and Drs. Carl Moos, and Mark Shoenberg for help, advice, and useful discussions during the course of this work. We are particularly indebted to Dr. H. A. Saroff for ideas about ion binding to muscle proteins. We thank Mrs. Dawn Collins for cheerful and willing technical assistance. We are also indebted to Dr. E. W. April for showing us his two manuscripts on crayfish muscle before publication.

Some early experiments were carried out in 1980 while one of us (G. F. Elliott) was visiting the State University of New York at Stony Brook. The visit was supported by a National Institutes of Health grant GM26392 to Dr. Maynard Dewey, whom we are very grateful to. Supported by S. E. R. C. Grant No. GRC 26521.

Received for publication 28 March 1984 and in final form 19 November 1984.

REFERENCES

Adams, M. J., A. Liljas, and M. G. Rossman. 1973. Functional anion binding sites in dog fish M_4 lactate dehydrogenase. *J. Mol. Biol.* 76:519–531.

Aldoroty, R. A., and E. W. April. 1984. Donnan potentials from striated muscle liquid crystals. A-band and I-band measurements. *Biophys. J.* 46:769–779.

Aldoroty, R. A., N. B. Garty, and E. W. April. 1985. Donnan potentials from striated muscle liquid crystals. Sarcomere length dependence. *Biophys. J.* 47:89–96.

Bartels, E. M., J. M. Skydsgaard, and O. Sten-Knudsen. 1979. The time course of the latency relaxation as a function of the sarcomere length in frog and mammalian muscle. *Acta Physiol. Scand.* 106:129–137.

Bartels, E. M., and G. F. Elliott. 1980. Donnan potential measurements in the A- and I-bands of cross-striated muscles and calculation of the fixed charge on the contractile proteins. *J. Muscle Res. Cell Mobil.* 1:452.

Bartels, E. M., and G. F. Elliott. 1981*a*. Donnan potentials from the A- and I-bands of skeletal muscle, relaxed and in rigor. *J. Physiol. (Lond.).* 317:85–87P.

Bartels, E. M., and G. F. Elliott. 1981*b*. Donnan potential measurements in the A and the I bands of barnacle muscle fibers under various physiological conditions. *J. Gen. Physiol.* 78:12*a*–13*a*. (Abstr.)

Bartels, E. M., and G. F. Elliott. 1982. Donnan potentials in rat muscle: difference between skinning and glycerination. *J. Physiol. (Lond.).* 327:72–73P.

Bartels, E. M., and G. F. Elliott. 1983. Donnan potentials in glycerinated rabbit skeletal muscle: the effect of nucleotides and of pyrophosphate. *J. Physiol. (Lond.).* 343:32–33P.

Bartels, E. M., P. H. Cooke, G. F. Elliott, and R. A. Hughes. 1985. Donnan potential changes in rabbit muscle A-bands are associated with myosin. *J. Physiol. (Lond.).* 358:80.

Bloomer, A. C., J. N. Champness, G. Bricogne, R. Staden, and A. Klug. 1978. Protein disk of TMV at 2.8 Å resolution showing the interactions within and between the subunits. *Nature (Lond.).* 276:362–368.

Cooke, P. H., E. M. Bartels, G. F. Elliott, and K. Jennison. 1984. Myosin threads. *Biophys. J.* 45 (2, Pt. 2):7*a*. (Abstr.)

De Simone, J. A. 1977. Perturbation in the structure of the double layer at an enzymic surface. *J. Theor. Biol.* 68:225–240.

Elliott, G. F. 1973. Donnan and osmotic effects in muscle fibers without membranes. *J. Mechanochem. Cell Motil.* 2:83–89.

Elliott, G. F., and C. R. Worthington. 1963. A small-angle optically focusing x-ray diffraction camera in biological research. Part I. *J. Ultrastr. Reson.* 9:166–170.

Elliott, G. F. 1980. Measurements of the electric charge and ion-binding of the protein filaments in intact muscle and cornea, with implications for filament assembly. *Biophys. J.* 32:95–97.

Elliott, G. F., and E. M. Bartels. 1982. Donnan potential measurements in extended hexagonal polyelectrolyte gels such as muscle. *Biophys. J.* 38:195–199.

Elliott, G. F., E. M. Bartels, P. H. Cooke, and K. Jennison. 1984. Evidence for a simple Donnan equilibrium under physiological conditions. *Biophys. J.* 45:487–488.

Elliott, G. F., J. Lowy, and C. R. Worthington. 1963. An x-ray diffraction and light diffraction study of the filament lattice of striated muscle in the living state and in rigor. *J. Mol. Biol.* 6:295–305.

Elliott, G. F., G. R. S. Naylor, and A. E. Woolgar. 1978. Measurements of the electrtic charge on the contractile proteins in glycerinated rabbit psoas using microelectrode and diffraction effects. *In* Ions in Macromolecular and Biological Systems. (Colston Papers No. 29). D. H. Everett and B. Vincent, editors. Scientechnica Press, Bristol, United Kingdom. 329–339.

Elliott, G. F., E. M. Rome, and M. Spencer. 1970. A type of contraction hypothesis applicable to all muscles. *Nature (Lond.).* 226:417–420.

El-Sach, S. C., and P. Johnson. 1982. Non-covalent binding of phosphate ions by striated muscle actin. *Int. J. Biol. Macromol.* 4:430–432.

Godt, R. E., and C. M. Baumgarten. 1984. Potential and K^+ activity in skinned muscle fibers. *Biophys. J.* 45:375–392.

Hanson, J. 1968. Recent x-ray diffraction studies of muscle. *Q. Rev. Biophys.* 1:177–216.

Harrington, W. F., K. Sutoh, and Y. Chen Chia. 1979. Myosin filaments and cross bridge movement. *In* Motility in Cell Function. F. A. Pepe, J. W. Sanger, and V. T. Nachmias, editors. Academic Press, Inc., New York. 69–90.

Huxley, H. E. 1968. Structural difference between resting and rigor muscle; evidence from intensity changes in the low-angle equatorial x-ray diagram. *J. Mol. Biol.* 37:507–520.

Huxley, H. E. 1973. Structural changes in the actin- and myosin-containing filaments during contraction. *Cold Spring Harbor Symp. Quant. Biol.* 37:361–376.

Jennison, K., G. F. Elliott, and C. Moos. 1981. Charge measurements of muscle proteins. *Biophys. J.* 33(2, Pt. 2):26*a*. (Abstr.)

Kensler, R. W., and M. Stewart. 1983. Frog skeletal muscle thick filaments are three-stranded. *J. Cell. Biol.* 96:1797–1802.

Koretz, J. F. 1982. Hybridization and reconstitution of thick-filament structure. *Methods Enzymol.* 85(B):20–31.

Kusmerick, M. J., and R. Podolsky. 1969. Ionic mobility in muscle cells. *Science (Wash. DC).* 166:1297–1298.

Loeb, G. I., and H. A. Saroff. 1964. Chloride and hydrogen-ion binding to ribonuclease. *Biochemistry.* 3:1819–1826.

Lowey, S., H. S. Slayter, A. G. Weeds, and H. Baker. 1969. Substructure of the myosin molecule. I. Subfragments of myosin by enzymic degradation. *J. Mol. Biol.* 42:1–29.

McLachlan, A. D., and J. Karn. 1982. Periodic charge distributions in the myosin rod amino acid sequence match cross-bridge spacings in muscle. *Nature (Lond.).* 299:226–231.

Milhayi, E. 1950. The dissociation curves of crystalline myosin. *Enzymologica.* 14:224–236.

Mobley, B. A., and B. R. Eisenberg. 1975. Size of components of frog skeletal muscle measured by methods of stereology. *J. Gen. Physiol.* 66:31–45.

Naylor, G. R. S. 1977. X-ray and microelectrode studies of glycerinated rabbit psoas muscle. Ph.D. thesis, The Open University, Milton Keynes, England. 147 pp.

Naylor, G. R. S. 1978. A simple circuit for automatic continuous recording of microelectrode resistance. *Pfluegers Arch. Eur. J. Physiol.* 378:107–110.

Naylor, G. R. S. 1982. On the average electrostatic potential between the filaments in striated muscle and its relation to a simple Donnan potential. *Biophys. J.* 38:201–204.

Naylor, G. R. S., E. M. Bartels, T. D. Bridgman, and G. F. Elliott. 1985. Donnan potentials in rabbit psoas muscle in rigor. *Biophys. J.* 48:47–59.

Orentlicher, M., J. P. Reuben, H. Grundfest, and P. W. Brandt. 1974. Calcium binding and tension development in detergent-treated muscle fibers. *J. Gen. Physiol.* 63:168–186.

Pemrick, S. M., and C. Edwards. 1974. Differences in the charge distribution of glycerol extracted muscle fibers in rigor, relaxation, and contraction. *J. Gen. Physiol.* 64:551–567.

Perutz, M. F. 1978. Electrostatic effects in proteins. *Science* (*Wash. DC*). 201:1187–1191.

Poulsen, F. R., and J. Lowy. 1983. Small-angle x-ray scattering from myosin heads in relaxed and rigor frog skeletal muscle. *Nature* (*Lond.*). 303:146–152.

Reedy, M. K., K. C. Holmes, and R. T. Tregear. 1965. Induced changes in orientation of the cross-bridges of glycerinated insect flight muscle. *Nature* (*Lond.*). 207:1276–1280.

Rome, E. 1972. Relaxation of glycerinated muscle: low-angle x-ray diffraction studies. *J. Mol. Biol.* 65:331–345.

Saroff, H. A. 1973. Action of hemoglobin. The energy of interaction. *Biopolymers.* 12:599–610.

Scordilis, S. P., H. Tedeshi, and C. Edwards. 1975. Donnan potential of rabbit skeletal muscle myofibrils I: electrofluorochromometric detection of potential. *Proc. Natl. Acad. Sci. USA.* 72:1325–1329.

Selveston, A. 1967. Structure and function of the transverse tubular system in crustacean muscle fibers. *A. Zoologist.* 7:515–525.

Worthington, C. R., and S. C. Liu. 1973. Structure of sarcoplasmic reticulum membranes at low resolution. *Arch. Biochem. Biophys.* 157:573–579.